Inelastic scattering of polarized protons from ^{4}He at 500 and 800 MeV

S. M. Sterbenz,* D. Dehnhard, M. K. Jones,† S. K. Nanda,‡ C. E. Parman, and Yi-Fen Yen
University of Minnesota, Minneapolis, Minnesota 55455

K. W. Jones and C. L. Morris
Los Alamos National Laboratory, Los Alamos, New Mexico 87545
(Received 23 May 1991)

Inclusive ^{4}He$(\vec{p},p')$ spectra were measured at incident energies $T_p = 500$ and 800 MeV over a range of forward scattering angles between 5° and 30°. The first excited 0^+, T=0 state at 20.1 MeV and the 2^-, T=0 state at 22.1 MeV appear as distinct structures in the spectra. Angular distributions of differential cross sections σ and analyzing powers A_y were extracted for these states and for regions of excitation in the continuum up to 40 MeV. Distorted-wave calculations for inelastic scattering using transition densities from the recoil corrected continuum shell model (RCCSM) were compared with the data. The RCCSM generally predicts too small σ and too large A_y. Assuming a pure giant monopole excitation for the 20.1-MeV, 0^+ state, we found greater giant monopole resonance strength than has been deduced from ^{4}He(e,e') studies.

PACS number(s): 25.40.Ep, 24.70.+s

I. INTRODUCTION

The mass-4 system is of fundamental interest in nuclear structure studies as the lightest system with a spectrum of known excited states. The excited states of ^{4}He in particular have received a great deal of attention in a number of different contexts. For example, controversial reports of photonucleon cross section ratios $R_\gamma = \sigma(\gamma,p)/\sigma(\gamma,n)$ of between 1.5 and 1.9 in the region of the giant dipole resonance (GDR) (summarized in Ref. [1]) have inspired many investigations in recent years. Such a large deviation from unity would have fundamental implications for the hadronic interaction, since it implies the existence of a charge symmetry-breaking (CSB) component of the internucleon force which, under standard assumptions, cannot be accounted for with the Coulomb interaction alone [1–3]. However, work involving separate measurements of the $\sigma(\gamma,p), \sigma(p,\gamma)$, and $\sigma(\gamma,n)$ reactions, as well as ^{4}He$(e,e'N)$ and pion inelastic scattering studies call these results seriously into question [4–8].

Pion inelastic scattering data have provided valuable information on the isospin character of the ^{4}He continuum and have also provided tests of microscopic approaches to the four-body nuclear structure problem [8]. Studies focusing on angular correlations in pion-induced proton knockout reactions have yielded π^+/π^- cross section ratios that are strongly dependent on excitation energy and correlation angle, and which do not appear to be understandable within the context of factorized distorted-wave Born approximation (DWBA) quasifree knockout theory [9, 10]. Apparently, the population and decay of the short-lived excited states of ^{4}He are also very important in the nucleon knockout process. Thus, a detailed account of the structure of these states is a prerequisite to understanding these data.

Another issue that has attracted interest recently is the structure of the 0^+ first excited state of ^{4}He at 20.1 MeV. Analysis of inelastic electron scattering experiments [11] has led to differing points of view on the nature of this state. In particular, the amount of $0s^{-1}\,1s$ giant monopole or "breathing mode" admixture in the 0^+ state has been reported to be quite small compared with two- and four-particle collective excitations to a deformed p shell [12]. However, calculations involving only one-particle–one-hole (1p-1h) excitations employing a realistic interaction and translationally invariant wave functions are also able to describe the measured longitudinal form factor without resorting to such a picture [13].

In this work, we report measurements of cross sections and analyzing powers (A_y) for inelastic proton scattering from ^{4}He to the continuum above 20 MeV in excitation energy. At proton bombarding energies of 500 and 800 MeV, the phenomenological nucleon-nucleon interaction is well known, and complete angular distributions for proton elastic scattering on ^{4}He have been measured [14–17]. With the essential ingredients for distorted-wave analysis thus provided, proton inelastic scattering at intermediate energies is a powerful tool for studying the structure of the ^{4}He continuum. We note that $(\vec{p},p')$ inelastic scattering measurements [18] in this range of ^{4}He excitation energies have also been carried out at lower bombarding energies (98.7 and 149.3 MeV), where the impulse approximation is less reliable.

*Present address: LAMPF, Los Alamos National Laboratory, Los Alamos, NM 87545.
†Present address: Rutgers University, Piscataway, NJ 08855.
‡Present address: CEBAF, Newport News, VA 23606.

 ©1992 The American Physical Society

We have found that proton scattering on ^{4}He is particularly favorable for studies of the first excited 0^+ and 2^- states, since these states emerge as distinct structures in the energy spectra. Other states form a broad continuum from which individual multipole strengths cannot be decomposed reliably. Analysis of our data has therefore proceeded along two lines. First, we have performed distorted-wave impulse approximation (DWIA) calculations for the 0^+ excitation. We have determined the amount of breathing mode strength necessary to account for the data and, in addition, have tested the treatment of the structure of this state given by the recoil corrected continuum shell model (RCCSM) [2, 13, 19, 20]. Second, we have carried out an extensive set of DWIA calculations using transition densities from the RCCSM for all of the multipolarities expected to contribute at given excitation energies. The summed predictions are compared with the continuum yields, binned in 2-MeV intervals. A similar procedure was followed in Ref. [8], where RCCSM predictions for the pion inelastic scattering yields were successful in reproducing excitation energy spectra.

As a part of the 500-MeV proton inelastic scattering experiment, we have also measured the spin-flip probability S_{nn} as a function of ^{4}He excitation energy at a single scattering angle 20°. The results of this measurement have been discussed elsewhere [21]. We note here that the spin response of the ^{4}He continuum, as established by this measurement, appears to be anomalous in the context of known spin-flip systematics [22]. In particular, values of S_{nn} larger than free nucleon-nucleon values and persisting to much higher excitation energies than expected either from systematics or from RCCSM predictions are seen in proton scattering on ^{4}He . The existence of such strong-spin collectivity provides further evidence that nuclear structure plays a critical role in the behavior of the continuum in the four-body system even for large values of missing mass.

II. THE EXPERIMENTS

The experiments were carried out with the High Resolution Spectrometer (HRS) [23] at the Los Alamos Meson Physics Facility (LAMPF) using 500- (494.0-) and 800- (800.0-) MeV polarized proton beams typically of 5–10 nA intensity, on a cooled ^{4}He gas target. ^{4}He($\vec{p}$,$\vec{p}'$) cross section and analyzing power data were taken at 500 MeV between laboratory scattering angles of 5° and 30° in 2.5° steps. At 800 MeV the data were taken between 6° and 20° in 2° steps. Beam polarization was always of the n type (perpendicular to the scattering plane), the direction of the proton's spin being reversed automatically at 3- to 5-min intervals for the analyzing power measurements.

The scattering angle acceptance of the HRS is 2.3° and the momentum acceptance, $\Delta p/p$, is approximately 3%. In the measurements at 500 MeV, three spectrometer field settings were required to cover a missing mass range of −10 to 55 MeV. For these three settings, the values of missing mass corresponding to central rays in the focal plane were 0, 27, and 45 MeV. (At 5° and 10° a measurement at 36 MeV was also taken for improved overlap between 27 and 45 MeV.) In the present analysis of the 500-MeV data, we have focused on the 27-MeV setting, as this covers the 17- to 37-MeV excitation energy region, where the most interesting structure in the ^{4}He continuum is found. However, we have also extracted elastic yields from the 0-MeV excitation bite and higher excitation continuum yields from the 45-MeV excitation bite. No distinct structures were found high in the continuum, either in σ or A_y. In the 800-MeV experiment, only one field setting was required, as this permitted measurements up to 35 MeV in missing mass. No elastic data were taken at this energy, but extensive elastic data already exist [15–17].

The standard arrangement for cross section and analyzing power measurements [23] at HRS was used in most of this work. The spin-flip probability measurements [21] on the ^{4}He($\vec{p}$,$\vec{p}'$) reaction at 20° at 500 MeV required, in addition, the use of the HRS focal-plane polarimeter [23] to determine the polarization of the outgoing protons. The target gas was contained in a nickel cylinder 5 cm

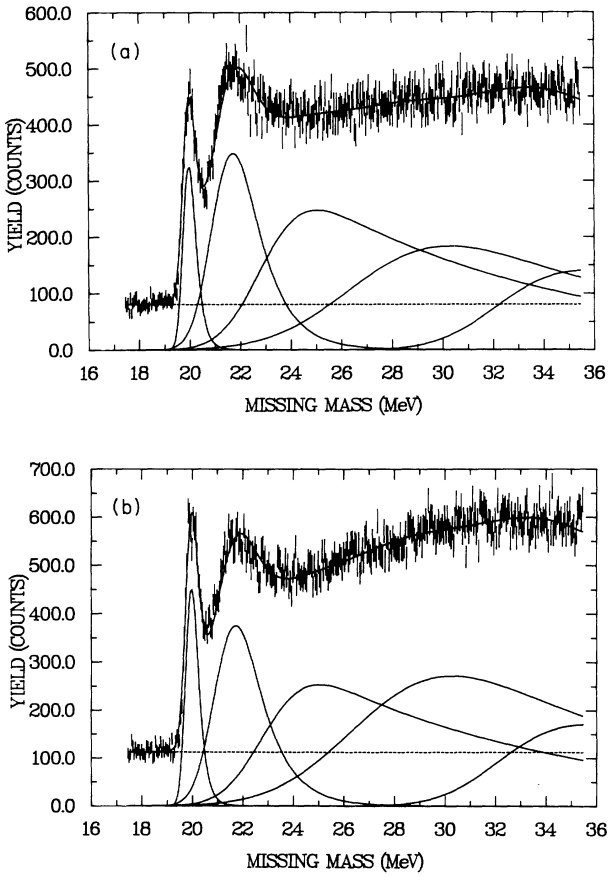

FIG. 1. Inclusive ^{4}He($\vec{p}$,p') missing mass spectra measured at 500 MeV, $\theta_{\rm lab}$= 20°. Top: normal polarization. Bottom: reverse polarization. Also shown are fits to the spectra to extract the yields for the 0^+ (20.1 MeV) and 2^- ($\approx$ 22 MeV) states. The broad structures with maxima near 25, 30, and 36 MeV were not used to extract yields but served to aid in estimating the contributions from the tails of the higher-lying continuum states to the 0^+ and 2^+ yields.

in diameter, cooled by liquid He to a temperature maintained at 9 to 10 K and pressurized to 1100 to 1150 torr. The effective areal density of the target was then approximately 30 mg/cm^2 (subject to variation as a function of scattering angle). In order to fix the absolute normalization, the gas target container was filled with H_2 gas and proton-proton elastic scattering data were taken at each angle. Absolute normalization factors were then determined by requiring reproduction of the $p+p$ elastic scattering cross sections from the most recent phase shifts of Arndt [24]. We monitored the ratio of pressure to temperature throughout the experiment in order to be able to correct for minor fluctuations in target thickness.

Figure 1 shows examples of spectra taken with normal and reverse polarization for 20° at 500 MeV. The sharper structure at lower energy is the 0^+ first excited state of ^{4}He at 20.1 MeV. The second distinct structure in the figure, about 2 MeV wide, corresponds to the 2^-, T=0 state which has been reported [25] at 22.1 MeV. At higher excitation energies, quasifree knockout and excitations of the 2^- (T=1), 1^- (T=0 and 1), and 2^+ (T=0) states are expected to contribute most of the strength. Although no distinct structures emerge in our experimental spectra above the 22.1-MeV 2^- state, the overall spectral shapes change markedly with angle.

III. DATA REDUCTION

A background arising from inelastic scattering from the target container is clearly visible as a plateau below the 0^+ state in Fig. 1. A reliable means of subtracting the contribution of this contaminant to the experimental spectra at 500 MeV was provided by empty target experiments, which were done at all scattering angles except 22.5° and 27.5° for the 27-MeV excitation bite. The background proved to be featureless and relatively constant over the entire missing mass range at all scattering angles except the two most forward: 5° and 7.5°, where the background rises toward smaller missing mass. Thus, in extracting yields for the 0^+ and 2^- states from our spectra, we have at most angles simply subtracted a constant background, the scale of which was fixed by the level of the plateau below threshold. The background shapes at 5° and 7.5° were determined from the corresponding empty target runs. At 800 MeV, no background measurements were made, but since the yield below the 0^+ state at 20.1 MeV was again constant as a function of missing mass, we followed the same procedure as for the larger angle 500-MeV data. The 500-MeV elastic scattering data were essentially free of contaminants and did not require background subtraction.

The elastic cross sections and analyzing powers at T_p = 500 MeV, obtained by use of normalization factors from the hydrogen target data, are shown in Fig. 2 and are compared with the measurements of Ref. [14]. We find that the analyzing power data are generally in good agreement. However, we also find that, although the two sets of cross-section data are consistent at angles of 20° and larger, there exists a discrepancy at smaller angles which grows systematically until, at 5° the present data are approximately 20% smaller than the older data. This discrepancy is not understood.

From the inelastic spectra, we first extracted yields for the two sharper states in the missing mass spectra: the 0^+ at 20.1 MeV and the 2^- at 22.1 MeV. Since the other, higher-lying states are so broad as to be impossible to unfold from each other in an unambiguous way, we also obtained total continuum yields, binned in 2-MeV energy intervals and background subtracted.

In order to extract yields for the two sharper states, it was necessary to take into account the yields contributed by the tails of the higher-lying broad states. This was done using the peak fitting code NEWFIT [26] according to the following procedure. We defined a set of five peaks with centroid locations and widths chosen to be consistent with values suggested by earlier studies [25, 8] for 0^+, 2^-, 1^-, 1^-, and 2^+ states. These parameters were permitted to vary within relatively narrow limits in such a way that the sum of the five line shapes fit the experimental missing mass spectra. The line shapes chosen in NEWFIT were exponential forms folded with Gaussians, the decay constant of the exponential being used to adjust the rate of falloff at higher energies. Each peak was characterized by four parameters: a centroid location, a width, a decay constant for the high energy tail, and

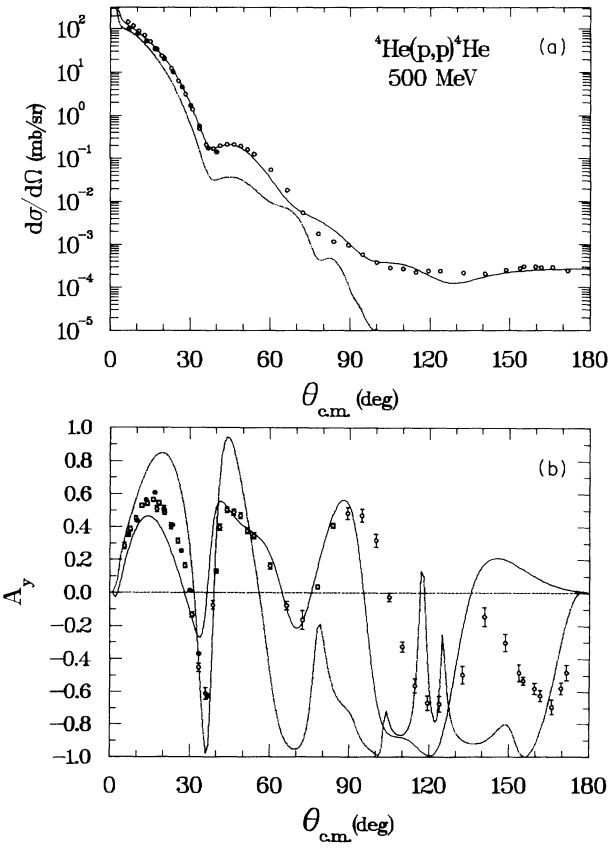

FIG. 2. Elastic scattering data for ^{4}He($\vec{p}$, p) at 500 MeV and optical potential calculations. Top: differential cross section. Bottom: analyzing power. Solid points: data of present work; open circles: data of Ref. [14]; solid line: phenomenological optical model fit; dashed line: folding model prediction.

an overall scale factor. A single set of line shapes was found that provided good fits to the entire set of 500- and 800-MeV data; only the scaling factor and a small energy offset (400 ± 150 keV to allow for beam energy and energy loss differences) were permitted to vary from spectrum to spectrum.

The results of the peak fitting for the spectrum taken at 20° and 500 MeV are shown in Fig. 1. We believe that the absolute yields derived for the 0^+ state by this method are accurate to within ±15%, while those for the 2^- state are only determinable within ±50%. These uncertainties are not included in the cross sections shown in Figs. 3–5. Although there must then be some question as to the overall scale for the 2^- data, we are confident that the relative yields, and therefore the angular distribution shapes, are determined to within systematic errors of not more than ±15% (statistical errors for the 2^- state were less than 1%, and those for the 0^+ state ranged from 2% to 5%). We exhibit the extracted cross sections for the 0^+ and 2^- excitations at 500 and 800 MeV in Figs. 3–5 with these ±15% error bars. Error bars shown for the analyzing powers are the statistical uncertainties only.

In our study of continuum yields, we binned each 500-MeV missing mass spectrum in 2-MeV intervals from 17 to 35 MeV. The first of these bins covers a range of effective excitation energies in ^{4}He in which no states are known. However, it furnishes a convenient means of background subtraction, since the yield in this bin arises entirely from scattering from the target container. Our procedure was to scale the binned empty target run yields by the foreground to background ratio in the 17- to-19-MeV bin and subtract the resulting yields from the binned foreground yields. This would provide a detailed account of the background shape at the scattering angles for which we had empty target data (all but 22.5° and 25°). Since the empty target background was found to be relatively constant, however, this procedure was essentially equivalent to subtracting a constant background as was done in the peak-fitting analysis.

Angular distributions of the continuum cross section and analyzing power extracted by this method for the eight excitation energy bins in the ^{4}He continuum are given in Figs. 6 and 7 along with RCCSM predictions for these observables (which we will discuss in Sec. V).

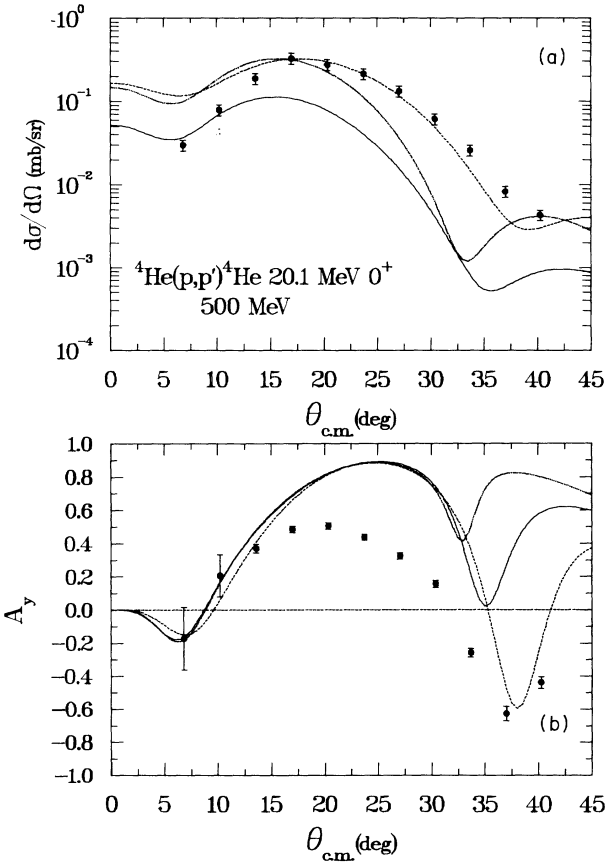

FIG. 3. Angular distributions for ^{4}He($\vec{p}$,p') inelastic scattering at T_p = 500 MeV to the 20.1-MeV, 0^+ state. Top: differential cross section. Bottom: analyzing power. Solid line: RCCSM prediction; dotted lines: pure GMR excitation from shell model prescription with c^2 = 0.23; dashed lines: pure GMR excitation using b_{eff} = 1.36 fm with c^2 = 0.27.

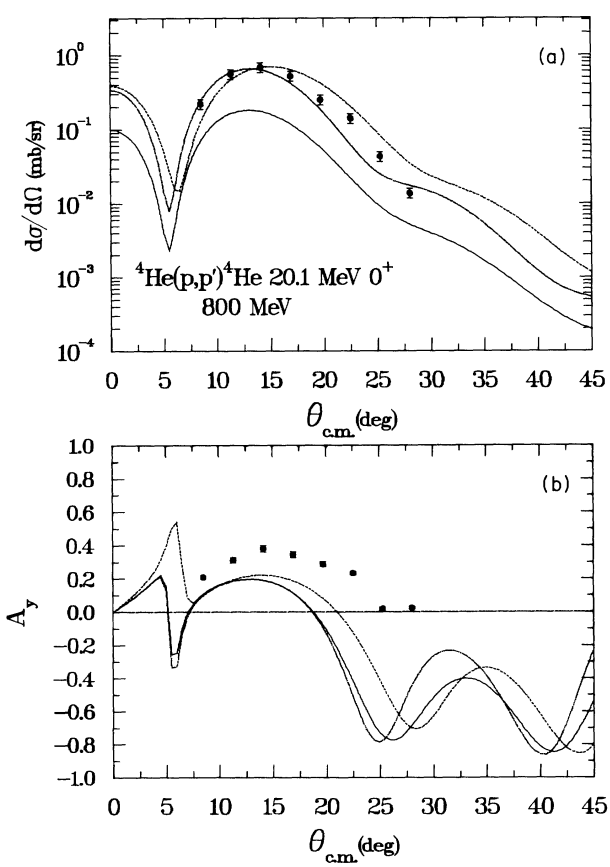

FIG. 4. Angular distributions for ^{4}He($\vec{p}$,p') inelastic scattering at T_p = 800 MeV to the 20.1-MeV, 0^+ state. Top: differential cross section. Bottom: analyzing power. Solid lines: RCCSM prediction; dotted lines: pure GMR excitation from shell model prescription with c^2 = 0.18; dashed lines: pure GMR excitation using b_{eff} = 1.36 fm with c^2 = 0.24.

IV. MODEL ANALYSIS OF INELASTIC TRANSITIONS

A. General remarks

Recently, the amount of giant monopole resonance (GMR) admixture in the first excited state of ^{4}He has been quite controversial. It has been pointed out by Liu and Zamick [12] that the magnitude of the measured longitudinal electron scattering form factor for the 0^+ state is too small to be consistent with the large GMR parentage which other studies have suggested [28]. It was shown that a $(0s)^3(1s)$ parentage of only 17% is sufficient to reproduce the scale of the data if a pure $(0s)^4$ ground state is assumed (revised by the authors in a private communication to us from the value of 4% given in Ref. [12]). The suggestion of Liu and Zamick is that contributions from 2p-2h and 4p-4h components of a deformed p shell are largely responsible for the low-lying positive-parity excited states of ^{4}He.

We have performed distorted-wave impulse approximation (DWIA) calculations for the 0^+ excitation in ^{4}He with two primary aims. Initially, a simple GMR exci-

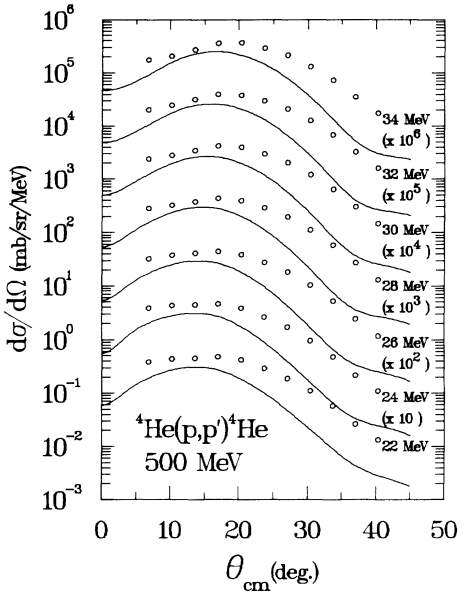

FIG. 6. Angular distributions of double differential cross section for ^{4}He($\vec{p}$,p') inelastic scattering at T_p = 500 MeV to the continuum in 2-MeV bites of excitation energy. The data are labeled by the excitation energy at the centers of their respective bins. Curves are DWIA calculations using RCCSM transition densities. The cross sections from all contributing multipolarities were summed.

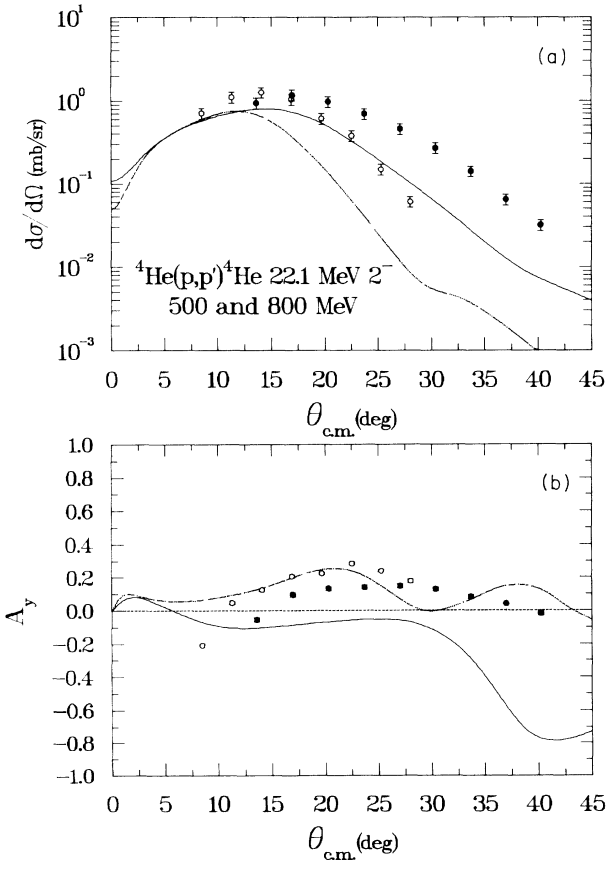

FIG. 5. Angular distributions for ^{4}He($\vec{p}$,p') inelastic scattering to the 22.1-MeV, 2^- state. Top: differential cross section. Bottom: analyzing power. Solid points: 500-MeV data; open circles: 800-MeV data; solid lines: 500-MeV DWIA calculation using RCCSM transition densities; dotted lines: 800-MeV DWIA calculation using RCCSM transition densities.

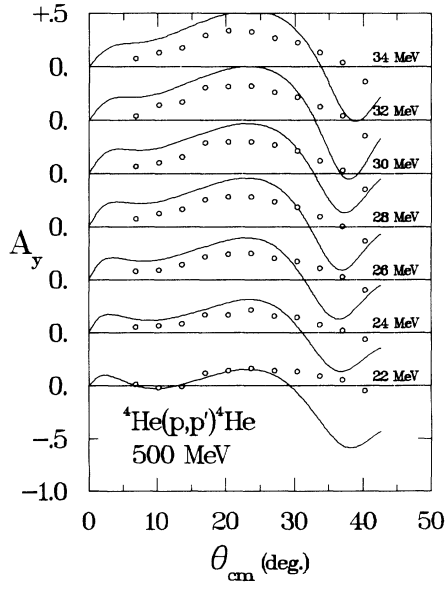

FIG. 7. Angular distributions of analyzing powers for ^{4}He($\vec{p}$,p') inelastic scattering at T_p = 500 MeV to the continuum in 2-MeV bins corresponding to those in Fig. 6. The curves are DWIA calculations using RCCSM transition densities. The calculated A_y from the contributing multipolarities were weighted by the corresponding cross sections.

tation was considered in order to obtain a comparison with the electron scattering results. Specifically, our interest was in determining what fraction of the full GMR strength was needed to reproduce the magnitude of the proton-induced 0^+ inelastic transition strength. In addition, we have carried out extensive DWIA calculations using full continuum wave function expansion coefficients from the RCCSM as a test of that model. Though unable to explain the anomalous ratio of photonucleon cross sections [1], this model has achieved notable successes in reproducing other data on the ^{4}He system. We note the attractive feature that, in this model, resonant excitations of ^{4}He and quasifree particle knockout are incorporated within the same theoretical framework. Low-energy cross sections, polarizations, and analyzing powers for the ^{3}H$(p,n)^3$He reaction, ^{3}H(p,γ) angular distributions, and inclusive π^+ and π^- scattering spectra [8] have been successfully described by the RCCSM [2, 19, 20].

Recently, the model has been applied to electron scattering data on the 0^+ first excited state as well [13], where it was demonstrated that 1p-1h excitations to higher-lying configurations, in addition to the GMR, can indeed account for the longitudinal form factor, and that the electron scattering data therefore do not require the involvement of multiparticle components in the 0^+ state. However, this model has not yet successfully described the transverse form factor from ^{4}He(e,e') studies, which is dominated by the spin excitations of the 1^- and 2^- states [27].

B. Analysis of (e,e') data with the GMR model

We have performed an analysis of the measured electron scattering form factor for the 0^+ state at 20.1 MeV following Ref. [12], in order to ensure consistency in our comparison of proton with electron scattering results. First, using the cross-section data from Ref. [11], we extracted the experimental form factor for the 20.1-MeV, 0^+ state directly. We then calculated a form factor using the simple model described below. The DWIA analysis of this work of the (p,p') data for this state is also based on this model.

The transition to the GMR may be represented as induced by the operator $r^2\,Y_{00}(\mathbf{r})$ and hence, in shell model terms, is a 1p-1h, $2\hbar\omega$ excitation. A calculation for pure GMR excitation is therefore straightforward if the ground state of ^{4}He is taken to be of $(0s)^4$ form. The GMR wave function is then just

$$\Psi_{\rm GMR} = \sqrt{3/4}\;|0s^{-1}1s> - \sqrt{1/4}\;|0s^{-2}0p^2>, \quad (1)$$

where the 2p-2h component is required to eliminate spurious center-of-mass excitation [29]. Since one-body interactions dominate in inelastic electron and intermediate energy proton scattering, model calculations for excitation of the 0^+ state by these means need only involve transition amplitudes of the form $0s$-ns. Therefore, barring fortuitous cancellations among transitions to higher s shells, we can place an upper limit on the GMR parentage of this state, following Liu and Zamick, by representing its wave function as follows:

$$\Psi_{20.1,\,0^+} = c\Psi_{\rm GMR} + d\Psi_{\rm multipart} \quad (2)$$

(where $c^2+d^2=1$). This simple model then involves only a single $0s$-$1s$ transition amplitude, and ignores transitions to higher s shells. Care is required in comparing calculations for proton and electron scattering when shell model transition densities are used, since the recoil correction required for shell model densities depends on the nature of the coordinate system employed in the scattering formalism.

In the plane-wave Born approximation (PWBA), the shell model form factor for an electron-induced transition between $0s$ and $1s$ harmonic oscillator basis states is given by [29]

$$F_L^{\rm SM}(q) = c'\sqrt{2/3}\,y e^{-y}, \quad (3)$$

where $y = q^2b_0^2/4$. Here, b_0 is the oscillator parameter, q is the momentum transfer, and $c' = c\sqrt{3/4}$ is the expansion coefficient for the $0s^{-1}1s$ part of the wave function of the 20.1-MeV, 0^+ state. The complete longitudinal form factor is then a product of three terms:

$$F_L(q) = f_{\rm c.m.}(q) f_N(q_\mu^2) F_L^{\rm SM}(q). \quad (4)$$

Here, $f_{\rm c.m.}=e^{y/A}$, a center-of-mass correction, and f_N is the proton form factor, given by

$$f_N(q_\mu^2) = [1 + q_\mu^2/(855\ {\rm MeV})^2]^{-2} \quad (5)$$

with q_μ denoting the four-momentum transfer.

The value of b_0 for ^{4}He was determined from the relation [30]

$$\langle r^2_{\rm point}\rangle = b_0^2\left(\sum_Q\left[Q\frac{z(Q)}{Z}\right] + \frac{3}{2}\frac{A-1}{A}\right), \quad (6)$$

where $\langle r^2_{\rm point}\rangle$ is the mean squared radius of the point nucleon density and $z(Q)$ is the number of protons in the major shell with $Q = 2n + l$ oscillator quanta ($n \geq 0$). If we assume a $0s^4$ ground state, $Q = 0$, and therefore $b_0 = \sqrt{8/9}\langle r^2_{\rm point}\rangle^{1/2}$. Then, using

$$\langle r^2_{\rm point}\rangle = \langle r^2_{\rm ch}\rangle - \langle r_p^2\rangle, \quad (7)$$

where $\langle r^2_{\rm ch}\rangle^{1/2} = 1.676$ fm [31] and $\langle r_p^2\rangle^{1/2} = 0.80$ fm are the rms charge radii of ^{4}He and the proton, respectively, we find $b_0 = 1.39$ fm.

In this simple degenerate harmonic oscillator model, c^2 is also the fraction of the non-energy-weighted $E0$ sum rule (NEWSR) consumed by this state, where

$$\text{NEWSR} = A\frac{e^2}{4}b_0^2\langle r^2_{\rm point}\rangle. \quad (8)$$

(Since only $2\hbar\omega$ excitations contribute to the sum rule, excitations to higher s shells do not contribute.) We note also that the energy-weighted $E0$ sum rule (EWSR) is simply this quantity multiplied by $2\hbar\omega$, and that, since

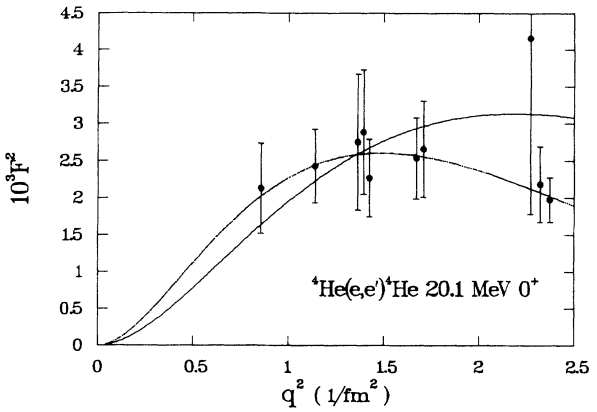

FIG. 8. Squared longitudinal form factor for inelastic electron scattering to the 20.1-MeV, 0^+ state in ^{4}He. Data from Ref. [11]. Solid curve: squared form factor calculated in GMR model with $c^2 = 0.17$ and $b_0 = 1.39$ fm; dotted curve: same as solid curve but with $c^2 = 0.12$ and $b_0 = 1.75$ fm.

$$\hbar\omega = \frac{(\hbar c)^2}{m_p c^2}\frac{1}{b_0^2}, \tag{9}$$

where m_p is the proton mass, the EWSR is in principle independent of b_0. If E_0=20.1 MeV is the true physical energy of the 0^+ state, $E_0c^2/(2\hbar\omega)$ is the fraction of the EWSR it consumes if we equate $B(E0 : 0s\text{-}1s)$ with $c\times$NEWSR. Taking $b_0 = 1.39$ fm, then $2\hbar\omega = 43$ MeV, and the fraction of the EWSR consumed is just $0.47c^2$. We note, however, that this result is then clearly not independent of b_0. Furthermore, the fact that $2\hbar\omega$ is so much larger than E_0 is itself an indication of the inadequacy of such a simple model, which treats all 0^+ states as degenerate.

The results of our electron scattering analyses are shown in Fig. 8. We find that with a value of $c^2 = 0.17$, the GMR model (solid line) reproduces the average scale of the experimental data, but that the shape of the form factor is reproduced so poorly that significantly different values of c^2 are conceivable. Of course, the rather poor statistics make a determination of what constitutes good reproduction of the data somewhat difficult here, but it is worth noting that only with the much larger value ($b_0 = 1.75$ fm) and the smaller value $c^2 = 0.12$ does this simple model yield a form factor (dotted line) which lies near the center of reasonable error bands. The electron data therefore do not support this simple model, and indicate that contributions from transitions involving either higher-lying s shells or g.s. correlations are very important. Nevertheless, the (e, e') data can be used to place a limit on the GMR strength in this state.

C. DWIA analysis of the (p, p') data

1. *Optical model analysis of the elastic data*

Differential cross sections for elastic scattering of protons from ^{4}He have been measured previously over the whole angular range, both at 500 MeV [14] and at 800 MeV [15–17]. We have obtained phenomenological optical potentials by fitting our forward angle data and the data of Ref. [14] at 500 MeV, and the data of Refs. [15, 17] at 800 MeV, using the optical potential search code RELOM [32]. At 500 MeV, where our cross-section data differ from those of the previous experiment [14] at the far forward angles, both data sets have been included in the fit. The optical potential parameters from the fits at the two energies are given in Table I.

Reproduction of the cross-section data at both energies is very good throughout the angular range of the measurements. Figure 2 shows the best-fit elastic cross sections and asymmetries (solid lines) along with the elastic scattering data at 500 MeV.

We also attempted to reproduce the elastic data with parameter-free folded optical potentials generated from the ground state (g.s.) nucleon point density of ^{4}He and the effective nucleon-nucleon (NN) interaction of Franey and Love [33, 34] (using the code ALLWORLD [35]). The g.s. point density was derived from the measured charge density [31] by unfolding the charge density of the proton, also with the code ALLWORLD [35]. The predicted observables (Fig. 2, dashed lines) differ significantly from the data except at the far forward angles at $\approx 10°$ and the position of the first minimum is reproduced quite well. Analyzing powers are only qualitatively reproduced at forward angles and not well described in any sense above 60°.

The failure of the folded potential to fit the elastic data is not unexpected. This potential is only the first-order term in the theoretical optical potential expansion. It has been shown by Feshbach *et al.* [36–39] that second- and third-order terms can be quite important. This was in fact demonstrated for 1-GeV proton scattering from ^{4}He. A calculation with the addition of higher-order terms to the folded optical potential, in order to improve the description of the elastic data, is beyond the scope of this

TABLE I. Optical potential parameters for elastic scattering of protons on ^{4}He at bombarding energies of 500 and 800 MeV. The central potentials have parts of Woods-Saxon shape $f(r, r_{V,W}, a_{V,W})$, with strengths V (real) and W (imaginary), and of (real) Woods-Saxon derivative shape with strength V_s, and geometry parameters r_s and a_s. The spin-orbit potentials are of Woods-Saxon derivative shape, i.e., $V_{s.o.}(r) = (V_{s.o.} + iW_{s.o.})(2/r)(d/dr)\ [f(r, r_{s.o.}, a_{s.o.})]\ \boldsymbol{l}\cdot\boldsymbol{\sigma}$. Potential depths are in MeV; geometry parameters are in fm.

T_p	V	r_V	a_V	W	r_W	a_W	V_s	r_s	a_s	$V_{s.o.}$	$r_{s.o.}$	$a_{s.o.}$	$W_{s.o.}$
500 MeV	-18.94	1.241	0.127	36.41	1.032	0.427	9.35	1.107	0.085	4.69	0.877	0.335	-3.71
800 MeV	43.17	0.663	0.188	73.80	1.008	0.384	-0.523	2.065	0.290	0.961	0.882	0.333	4.66

work, inasmuch as we are primarily concerned with forward angle inelastic scattering.

In the analysis that follows (next section), we have used the standard procedure of generating distorted waves for the DWIA calculations from the phenomenological optical potentials obtained from the fit to the elastic data. In order to check the sensitivity to the choice of the optical potential, we have also done some DWIA calculations with the folded potential. We found that the absolute inelastic peak cross sections predicted by the phenomenological potential differed by only $\approx 5\%$ from the prediction with the folded potential in the region of momentum transfer where we measured the cross sections. The angular distribution shapes do not differ very much either. Since the phenomenological potential calculation is expected to be closer to the prediction from a many-order optical potential than from a first-order one, we believe that a conservative estimate of the uncertainty in the absolute cross sections due to the use of the fitted potential is even less than 5%. Differences of this order have a negligible impact on the conclusions of our analysis, especially when compared with other model uncertainties that we will discuss.

2. *DWIA analysis of 0^+ state with the GMR model*

The DWIA calculations were carried out with a modified version [40,41] of the program DWBA70, using the distorted waves from the phenomenological optical potential, the Franey-Love NN interaction [33,34] to calculate the effective proton-nucleus interaction (which causes the inelastic transition), and the transition densities produced from harmonic oscillator wave functions.

It is important to note that a correct determination of the coefficient c of Eq. (2) from the Z coefficient used in DWBA70 for the $0s$-$1s$ transition amplitude requires that the difference between shell model and DWIA coordinate systems be taken into account. This can be done in an approximate manner by applying a correction factor to the shell model one-body density matrix element (OBDME) and by using, simultaneously, an effective oscillator parameter to construct the DWIA transition densities [42, 43]. In particular, if α represents the shell model OBDME (which in this model is $\sqrt{3/4}$), the corresponding Z coefficient is

$$\alpha\left(\frac{A}{A-1}\right)^{(Q_1+Q_2)/2} \tag{10}$$

where Q_1 and Q_2 are the principal quantum numbers $(2n+l)$ for initial and final states, respectively. Here we have $Q_1 = 0$ and $Q_2 = 2$ with $A = 4$, and so the Z coefficient corresponding to a value of unity for c is just $\sqrt{4/3}$. The effective oscillator parameter is given by

$$b_{\text{eff}} = b_0\sqrt{\frac{A}{A-1}} \tag{11}$$

or $b_{\text{eff}} = 1.60$ fm for ^{4}He with $b_0 = 1.39$ fm, the value derived from the ground-state charge density.

The results of the DWIA calculations for the 20.1-MeV state following these prescriptions are compared with the proton inelastic scattering data at $T_p = 500$ and 800 MeV in Figs. 3 and 4, respectively (dotted lines). Also plotted in these figures are calculations with $b_{\text{eff}} = 1.36$ fm (dashed lines). (The solid lines will be discussed in the next section.) This value of b provided the best compromise in angular distribution shape at the two different bombarding energies. Our aim in using this value was to test the level of sensitivity of our model calculations to the value of b.

We note that at 800 MeV the angular distribution shape is fitted quite well by the simple model calculation, but that at 500 MeV the diffraction pattern is too narrow relative to the data. This may simply reflect the failure of such a simple model to describe the 0^+ excitation, but a qualitatively similar "diffraction shift" phenomenon has also been noted in the systematics of elastic proton scattering on nuclear targets at intermediate energies [44].

The calculations give the correct sign for the analyzing powers at forward angles, but generally overestimate them at 500 MeV and underestimate them at 800 MeV. With $b_{\text{eff}} = 1.36$ fm, the DWIA calculation very nearly reproduces the zero crossing and the minimum in the 500-MeV analyzing power, but none of the calculations is particularly successful in this regard at 800 MeV.

The Z coefficients used in these calculations were scaled so that the maximum of the calculated cross section coincided with that of the data. Values for c^2 determined from these coefficients by the relation given above were as follows: (1) with $b_{\text{eff}} = 1.60$ fm, $c^2 = 0.23$ at 500 MeV and 0.18 at 800 MeV; (2) with $b_{\text{eff}} = 1.36$ fm, $c^2 = 0.27$ at 500 MeV and 0.24 at 800 MeV. Thus, we find that all of the values of the fraction of the NEWSR consumed by the 0^+ first excited state of ^{4}He are larger than the value of 17% of the full GMR strength deduced from the electron scattering form factor.

Of course, this comparison must be tempered with an acknowledgement of the various uncertainties involved. In particular, the poor statistics of the electron data, departures of the measured q or angle-dependent shapes from those given by the calculations, and differences in the methods used to separate the 0^+ yield from the underlying continuum all contribute uncertainties that are important at the level of this comparison. (We remark that a smooth continuum background was also subtracted from the 0^+ yield in the electron study [11].)

3. *Analysis of the 0^+ state with the RCCSM*

The RCCSM provides a description of nuclear states with one particle in the continuum which is free of spurious center-of-mass motion—an especially important consideration in very light systems such as ^{4}He. In applying the model to the four-nucleon problem, Halderson *et al.* [2, 13, 19, 20] have used the effective G-matrix interaction of Bertsch *et al.* [45] and allowed excitations of 1p-1h character. The RCCSM representation of continuum states uses a basis of harmonic oscillator states defined with respect to a set of Jacobi coordinates invariant under translations of the center of mass. For DW calculations, the model provides complex, excitation-energy-

dependent, wave-function expansion coefficients in terms of these basis states.

Since the transition densities used in the DWBA70 code are, however, referred to a center-of-mass radial coordinate rather than the Jacobi coordinate used in the RCCSM, recoil correction factors had to be applied to the oscillator parameter and radial integration grid [27]. A b_0 value of 1.66 fm had been used in earlier RCCSM calculations which correctly gave the ^{3}H elastic electron scattering form factor at low q. This corresponds to a b_{eff} of 1.92 fm for use in DWBA70. In addition, the radial integration grid had to be scaled by a factor $A/(A-1) = 4/3$.

In the calculations reported here, as in the work of Refs. [2, 8, 19, 20], the ground state of ^{4}He is assumed to be of purely $(0s)^4$ form. The basis for the excited 0^+ state consists of higher s orbitals up to $n = 8$. RCCSM expansion coefficients for the $p+t$ and $n+^3$He exit channels are provided on a grid of excitation energies extending from the appropriate particle threshold to 30 MeV, but 70% of the 0^+ transition strength is concentrated within about 1 MeV of the lower limit. Since our data are inclusive measurements from which only total 0^+ yields were extracted, it was necessary to add the calculated cross sections (or cross-section–weighted spin observables) for the $p+t$ and $n+^3$He channels incoherently at each excitation energy and then integrate over the region of excitation energy spanned by the experimental 0^+ peak (threshold to 22 MeV).

We carried out full direct plus exchange DWBA70 calculations using the four components of the Franey-Love NN force which contribute to the excitation of the 0^+ state. (The real and imaginary central and spin-orbit forces contribute; the tensor force does not.) We did this for the real and imaginary RCCSM expansion coefficients separately, retaining the resulting eight sets of amplitudes for multiplication by the appropriate phase before adding them coherently.

The results of these calculations for 500- and 800-MeV proton scattering are shown compared with our data and the other calculations in Figs. 3 and 4 (solid lines). The RCCSM predictions are considerably smaller than the measured cross sections at both energies, though at 800 MeV the difference is smaller and the angular shape is reasonably well reproduced. It is important to note, however, that in a recent successful application [13] of the RCCSM to the electron scattering data for the excited 0^+ state in ^{4}He, the ground state contained a 17% admixture of $(ns)^1(0s)^{-1}$ correlations and the description of transitions to the excited states included additional recoil corrections. Furthermore, we have found that DWBA calculations using the RCCSM prescriptions with only the giant monopole component $(1s^10s^{-1})$ of the full transition density yielded much larger cross sections than our complete calculation. Thus, the results reported here appear to depend rather critically on cancellations among the various amplitudes used to generate the transition densities. It is, therefore, possible that the inclusion of ground-state correlations in the RCCSM description of the ^{4}He system would have a large effect on the overall magnitude of the cross sections.

The analyzing power calculations appear to be more sensitive to the radial extent of the transition density than to the Z coefficients, since the angle-dependent shapes of the A_y using RCCSM amplitudes do not differ dramatically from those given by the other calculations shown in Figs. 3 and 4. We found that the quantity b_{eff} is more important to the angular distribution of A_y than are the transition amplitudes. This observable thus appears more useful as a test of the DWIA formalism embodied in DWBA70 than a means of differentiating models of ^{4}He structure.

4. Analysis of the 2^- state and the continuum with the RCCSM

We have also applied the RCCSM transition densities to DWIA calculations of cross sections and analyzing powers for the energy-binned continuum at T_p = 500 MeV, and for the transition to the 2^-, T=0 state at 22.1 MeV at both T_p = 500 and 800 MeV. Although in the calculation of summed continuum yields one loses the ability to test the model's description of the excitation of specific multipolarities, a beneficial characteristic of this approach is that the ambiguity implicit in any attempt to disentangle them from each other in the experimental data also vanishes.

We have carried out DWBA70 calculations with RCCSM expansion coefficients at seven excitation energies corresponding to the central energies of the continuum data bins from 22 to 34 MeV. Cross sections for 0^+, 2^-, 1^-, and 2^+ multipole strengths were obtained simply by addition, and continuum asymmetries were obtained by weighting those of the individual multipoles by cross section to give quantities that could be compared directly with the 500-MeV continuum data. We also calculated σ and A_y at both 500 and 800 MeV for the 2^- excitation alone, integrating over excitation energies from threshold to 26 MeV.

The RCCSM explicitly distinguishes between the two possible angular momentum couplings of the unbound nucleon ($J = L \pm S$). Therefore, DWIA calculations for states other than the 0^+ state involve the incoherent addition of observables for four physically distinguishable exit channels instead of the two required for the 0^+ excitation, where $L = 0$. As before, all excitations are of 1p-1h character from a $(0s)^4$ ground state, but the number of expansion coefficients is typically much larger for the 2^-, 1^-, and 2^+ excitations because of the multiplicity of possible couplings. The entire set of calculations required approximately three CPU hours on the Cray-2 computer of the Minnesota Supercomputer Institute.

We compare the results of these calculations with energy-binned continuum data in Figs. 5, 6, and 7. We find that, at the angular distribution maxima, the calculated cross sections are within a factor of 2 of the data. However, calculations and data differ in diffractive structure, the calculations having maxima at smaller angles. This is analogous to the situation for the 0^+ excitation at 500 MeV. Again, it appears that destructive interference among the many amplitudes brings about a reduction in

the overall scale of the cross section. The effect of correlations in the ground state is not known, but may be very significant.

Measured analyzing powers (Fig. 7) for the summed continuum yield are reproduced quantitatively at forward angles and at smaller excitation energies. At higher excitation energies, the calculated analyzing powers are generally too large in absolute magnitude, but the qualitative trends of the data are reflected in the calculations. However, A_y for the 2^- excitation is not at all well described by these calculations (Fig. 5).

V. SUMMARY AND CONCLUSIONS

We have measured excitation energy spectra for the ^{4}He$(\vec{p},p')$ reaction at 500 and 800 MeV over a range of forward scattering angles and have extracted angular distributions for inelastic scattering to the first 0^+ and 2^- states of ^{4}He. From the 500-MeV spectra we have also extracted angular distributions of energy-binned continuum yields. We have carried out DWIA analyses of these data using amplitudes from the RCCSM and from a simple model where the 0^+ state is described as a pure GMR excitation in order to gain a comparison with results from electron scattering studies.

A persistent feature emerging from our analyses is that the assumption of pure $(0s)^4$ structure in the ground state of ^{4}He is not justified. This idea has been borne out in recent successful RCCSM calculations [13] of the inelastic electron scattering form factor for the first excited 0^+ state of ^{4}He.

Distorted wave calculations for inelastic scattering to the 0^+ first excited state of ^{4}He with both 500- and 800-MeV protons were carried out with pure giant monopole transition amplitudes. These calculations indicate a maximum GMR parentage of 18% to 27%, depending on the beam energy considered and the oscillator parameter used. This is somewhat larger than the limit obtained from a similar analysis of the longitudinal electron scattering form factor for this transition.

A RCCSM description of the 0^+ excitation that does not include ground-state correlations predicts cross sections for this state that are too small by factors of 5 or more. Apparently, the shortage in cross section arises from cancellations among the many contributing amplitudes. It would be interesting to investigate the effect of including ground-state correlations on the RCCSM predictions for proton scattering from ^{4}He.

For excitations higher in the continuum, the RCCSM predictions without ground-state correlations are much closer to the data, but still there is a shortage of yield, the continuum cross sections at 500 MeV underpredicted by about a factor of 2 at the maxima. Also, the model does not predict a distinct structure corresponding to that seen around 22 MeV in our data, which one would expect to arise predominantly from the 2^-, T=0 state expected at 22.1 MeV [25]. We have found that continuum analyzing powers are reasonably well reproduced qualitatively and, for the lower half of excitation energies and angles in our data, even quantitatively.

It is interesting to note, however, that the analyzing powers we calculate using the code DWBA70 with amplitudes from the RCCSM are generally too large at higher excitation energies, while the spin-flip probabilities S_{nn} compared with our measurements at 20° using 500-MeV protons are too small. Our calculations give values for S_{nn} here which, above 30 MeV in excitation, tend rapidly toward the averaged free NN values, in agreement with expectations based on systematic studies of S_{nn} as a function of target and incident energy [21,22]. The much larger measured values represent a significant anomaly in the systematics of the spin response of nuclear systems.

Our data on the excitation of the ^{4}He continuum with intermediate energy proton probes allow extensive tests of models of few-body systems. The RCCSM—the best semimicroscopic treatment of this system currently available to us for use in DWIA calculations—does not provide a fully successful description of these data. A relativistic DWIA treatment might improve the agreement with the data, particularly with the spin observables.

ACKNOWLEDGMENTS

The authors are indebted to Dr. M. A. Franey, Prof. D. Halderson, and Dr. A. C. Hayes for numerous useful discussions. The authors also acknowledge the receipt of a generous grant for computing time from the Minnesota Supercomputer Institute. This work was supported in part by the U.S. Department of Energy.

[1] J. R. Calarco, B. L. Berman, and T. W. Donnelly, Phys. Rev. C **27**, 1866 (1983).
[2] Dean Halderson and R. J. Philpott, Phys. Rev. C **28**, 1000 (1983).
[3] F. C. Barker, Aust. J. Phys. **37**, 583 (1984).
[4] R. Bernabei *et al.*, Phys. Rev. C **38**, 1990 (1988).
[5] D. J. Wagenaar, N. R. Robertson, H. R. Weller, and D. R. Tilley, Phys. Rev. C **39**, 352 (1989).
[6] K. Maeda (Tohoku Univ., Japan), private communication (1988).
[7] M. Spahn *et al.*, Phys. Rev. Lett. **63**, 1574 (1989).
[8] C. L. Blilie, D. Dehnhard, D. B. Holtkamp, S. J. Seestrom-Morris, S. K. Nanda, W. B. Cottingame, D. Halderson, C. L. Morris, C. Fred Moore, P. Seidl, H. Ohnuma, and K. Maeda, Phys. Rev. Lett. **57**, 543 (1986).
[9] Mark K. Jones, Ph.D. dissertation, Univ. of Minnesota (1989); Los Alamos National Laboratory Internal Report LA-12015-T, 1991.
[10] M. K. Jones *et al.*, Phys. Rev. C **42**, R807 (1990).
[11] G. Köbschall *et al.*, Nucl. Phys. **A405**, 648 (1983).
[12] H. Liu and L. Zamick, Phys. Rev. C **33**, 1093 (1986).
[13] D. Halderson, Ming Yu, and Jiang Yu, Phys. Rev. C **39**, 336 (1989).
[14] G. A. Moss *et al.*, Phys. Rev. C **21**, 1932 (1980).
[15] J. Fong *et al.*, Phys. Lett. **78B**, 205 (1978).
[16] H. Courant *et al.*, Phys. Rev. C **19**, 104 (1979).
[17] G. N. Veleckov *et al.*, Yad. Fiz. **42**, 1325 (1985) [Sov. J.

Nucl. Phys. **42**, 837 (1985)].
[18] J. S. Wesick *et al.*, Phys. Rev. C **32**, 1474 (1985).
[19] Dean Halderson and R. J. Philpott, Nucl. Phys. **A321**, 295 (1979).
[20] Dean Halderson and R. J. Philpott, Nucl. Phys. **A359**, 365 (1981).
[21] S. K. Nanda, S. M. Sterbenz, D. Dehnhard, M. K. Jones, Yi-Fen Yen, and K. W. Jones, in *Proceedings of the 8th International Symposium on High Energy Spin Physics, Minneapolis, MN, 1988*, edited by K. J. Heller, AIP Conf. Proc. No 187 (AIP, New York, 1989), p. 681.
[22] S. Nanda *et al.*, Phys. Lett. **188**, 177 (1986).
[23] Sirish K. Nanda, Ph.D. dissertation, Rutgers Univ. (1985); Los Alamos National Laboratory Internal Report LA-10368-T, 1985.
[24] Arndt, computer code SCATTERA (solution SM89), 1989 (unpublished).
[25] S. Fiarman and W. E. Meyerhof, Nucl. Phys. **A206**, 1 (1973).
[26] C. L. Morris, computer code NEWFIT, 1989 (unpublished).
[27] A. Hotta, J. Dubach, R. S. Hicks, R. L. Huffmann, B. Parker, G. A. Peterson, R. J. Ryan, R. P. Singhal, and D. Halderson, Phys. Rev. C **38**, 1547 (1988); Dean Halderson, private communication (1988).
[28] J. Carvalho and D. Rowe, Nucl. Phys. **A465**, 265 (1987).
[29] Anna Hayes, private communication (1990).
[30] S. Chakravarti, D. Dehnhard, M. A. Franey, S. J. Seestrom-Morris, D. B. Holtkamp, C. L. Blilie, A. C. Hayes, C. L. Morris, and D. J. Millener, Phys. Rev. C **35**, 2197 (1987).
[31] H. De Vries, C. W. De Jager, and C. De Vries, At. Data Nucl. Data Tables **36**, 495 (1987).
[32] M. A. Franey, computer code RELOM, based on computer code RAROMP by G. J. Pyle (unpublished).
[33] W. G. Love and M. A. Franey, Phys. Rev. C **24**, 1073 (1981).
[34] M. A. Franey and W. G. Love, Phys. Rev. C **31**, 488 (1985).
[35] J. Carr, F. Petrovich, and J. Kelly, computer code ALLWORLD (unpublished).
[36] H. Feshbach and J. Hüfner, Ann. Phys. (N.Y.) **56**, 268 (1970).
[37] H. Feshbach, A. Gal, and J. Hüfner, Ann. Phys. (N.Y.) **66**, 20 (1971).
[38] E. Lambert and H. Feshbach, Ann. Phys. (N.Y.) **76**, 80 (1973).
[39] J. J. Ullo and H. Feshbach, Ann. Phys. (N.Y.) **82**, 156 (1974).
[40] R. Schaeffer and J. Raynal, computer code DWBA70 (unpublished).
[41] M. A. Franey, modifications to computer code DWBA70 by R. Schaeffer and J. Raynal (unpublished).
[42] D. J. Millener, J. W. Olness, E. K. Warburton, and S. S. Hanna, Phys. Rev. C **28**, 497 (1983).
[43] F. P. Brady, T. D. Ford, G. A. Needham, J. L. Romero, E. L. Hjort, D. Sorenson, C. M. Castaneda, J. L. Drummond, B. McEachern, N. S. P. King, and D. J. Millener, Phys. Rev. C **43**, 2284 (1991).
[44] L. Ray and G. W. Hoffmann, Phys. Rev. C **31**, 538 (1985).
[45] G. Bertsch, J. Borysowicz, H. McManus, and W. G. Love, Nucl. Phys. **A284**, 399 (1977).